NASA Contractor Report 198280

ICASE Report No. 96-9

ICASE

ON THE EFFECT OF FEEDBACK CONTROL ON BÉNARD CONVECTION IN A BOUSSINESQ FLUID

Trudi A. Shortis
Philip Hall

NASA Contract No. NAS1-19480
February 1996

Institute for Computer Applications in Science and Engineering
NASA Langley Research Center
Hampton, VA 23681-0001

Operated by Universities Space Research Association

National Aeronautics and
Space Administration

Langley Research Center
Hampton, Virginia 23681-0001

On the effect of feedback control on Bénard convection in a Boussinesq fluid

Trudi A. Shortis
Department of Mathematics
University of Manchester
Manchester M13 9PL, U.K.
and
Philip Hall
Department of Mathematics
University of Manchester
Manchester M13 9PL, U.K.

Abstract

The effect of nonlinear feedback control strategies on the planform of convection in a Boussinesq fluid heated from below is investigated. In the absence of the control, given that non-Boussinesq effects may be neglected, it is well known that convection begins in the form of a supercritical bifurcation to rolls. Non-Boussinesq behaviour destroys the symmetry of the basic state, and through a subcritical bifurcation leads to the formation of hexagonal cells. Here we discuss the influence of regulation of the lower surface temperature by means of a control mechanism, made up of a combination of a proportional linear and nonlinear controller, on the stability of the hexagonal cell pattern.

[1]This research was supported in part by the National Aeronautics and Space Administration under NASA Contract No. NAS1-19480 while the second author was in residence at the Institute for Computer Applications in Science and Engineering (ICASE), NASA Langley Research Center, Hampton, VA 23681-0001. Support for the first author was provided by EPSRC, UK.

1 Introduction

Our concern is with the effects of feedback control on the evolution of convective instabilities in a Boussinesq fluid heated from below. The stability of Bénard convection is of both mathematical and physical importance, and is of particular relevance to material processing applications, where it is often more desirable to operate at Rayleigh numbers in excess of the critical value above which thermal convection normally occurs, but in the absence of such convective instabilities.

Currently methods for suppressing convection include, damping fluid motion in electrically conducting materials with magnetic fields, and also operating in a reduced gravity environment in order to minimise the effects of buoyant convective currents.

It is well known, that for non-Boussinesq fluids, where variation of temperature with viscosity is taken into account, the onset of convection in a steady fluid layer, heated from below, takes the form of hexagonal cells with the flow direction at the cell centre determined by the sign of the change in sign in viscosity variation. (See Segel & Stuart (1962), Palm et al. (1967), Segel (1965), and Busse (1967).) This cell pattern is induced by a subcritical bifurcation to convective rolls. Further increase in the Rayleigh number cause a destabilisation of the hexagonal pattern, and roll modes are established. However, if the Rayleigh number is subsequently decreased to a value below that at which the roll modes first appeared, hysteresis effects are seen, that is, the hexagonal cells are not re-established until a value below that at which transition to the roll mode first occurred. This is a consequence of the subcritical bifurcation, and an additional consequence due to the nature of this bifurcation is that the onset of convection occurs discontinuously when the Rayleigh number is increased.

Considerable research has been done on stratagies to delay the onset of Bénard convection in a fluid layer heated from below and/or cooled from above through modulation of the boundary conditions and, in particular, the time-periodic modulation of the temperature difference across the layer - see Davis (1976), and Donnelly (1990). Previous authors have found that this leads to a small increase in the critical Rayleigh number (see Meyer, Cannell and Ahlers (1992)). However, Roppo, Davis & Rosenblat (1984), found that periodic modulation of the lower surface temperature induces symmetry breaking effects sufficient to cause a subcritical bifurcation and thus the no-motion state may only be stable for small perturbations.

Recently, Kelly and Hu (1993), showed that a time-periodic non-planar shear flow significantly stabilises the Bénard problem. In a subsequent paper Hall and Kelly (1995), it was found that steady and unsteady shear flows removed the preference for hexagonal cells at the onset of convection in a non-Boussinesq fluid. This was achieved by sufficiently splitting apart the critical Rayleigh numbers for each member of a triad of roll disturbances which interact to produce the hexagonal cells.

The mechanism found by Kelly and Hu (1993), is possibly explained by results for convection in unidirectional steady flows, see the review by Kelly (1993), and this possi-

bility is summarised in Hall (1995). Kelly and Hu found that the maximum stabilising effects were for low frequencies. For this reason, Hall (1995) concentrated on the low frequency regime, and investigated the interactions between all possible roll disturbances for a given value of the Rayleigh number. Note that for small amplitude unsteady flows, subcritical convection of any form is not possible, Hall and Kelly (1995), which is in contrast to the results of Roppo, Davis and Rosenblat (1984). Hall (1995), found that there exists a threshold frequency, below which imperfections in the system play a crucial role, causing the system to respond in a quasi-steady manor. The non-linear problem becomes singular, in the sense that, the solution to the problem differs by an $O(1)$ amount from the imperfection free solution. However, even for frequencies small enough to induce quasi-steady behaviour within the fluid layer, at any instant in time the convection cells do not line up with the direction identified as most unstable on the basis of linear theory, that is, the behaviour for such frequencies cannot be predicted from the corresponding steady case. The convection patterns in this regime are found to change with time, and are extremely complicated with straight rolls existing only for part of a period. It was also found that the Kelly-Hu mechanism persists into the nonlinear regime until imperfections start to play a role in the system. Thus practical application of such a stabilising method must ensure that the frequency of the oscillations required for a full stabilising effect is shorter than that over which imperfections have an effect on convection. In addition, the necessary horizontal motions may also have an adverse effect in materials processing.

In various experimental and theoretical investigations, by Singer, Wang and Bau, (see references), the bifurcation structure associated with convection has been successfully changed by means of a feedback controller in a thermal convection loop, heated from below and cooled from above. Thus the Rayleigh number above which convective motion occurs was higher than that for the uncontrolled system. In addition, they also induced chaotic behaviour for flows which would otherwise be laminar.

Tang and Bau (1993), implemented similar ideas when investigating the Lapwood problem for a horizontal saturated porous layer, confined in a box heated from below, and cooled from above. Lapwood convection is relevant to transport processes in the mushy region of solidification, and also in thermal porous insulators. The convection in such a medium, may be modelled for low to moderate Darcy-Rayleigh numbers by the Darcy-Oberbeck-Boussinesq equations. They concluded that the no-motion state could be maintained by means of feedback control strategies, for Rayleigh numbers exceeding the critical values for the uncontrolled system. In addition, the control mechanism was found to leave unaltered the no-motion solution of the classical equations, but changes the stability characteristics by altering the system dynamics. The control mechanism implemented was either of the proportional, or differential kind or a combination of the two.

The problem under investigation here, concerns the effects of a nonlinear feedback control mechanism, that is we modulate the lower surface thermal boundary conditions with reference to the midlayer temperature with a combination of proportional and non-

linear controllers, the latter being dependent on the square of the reference temperature.

The aim of this study is to determine firstly if subcritical convection can take place, and investigate the stability when nonlinear effects are taken into account.

In the first instance, we shall derive a system of amplitude equations, which are generalisations of those found by Segel (1965), for the problem under consideration. In section 3, we will investigate the bifurcation structure of these equations. And finally, in section 4 we shall draw some conclusions.

2 Formulation

Consider a fluid occupying the region $0 < z < d$, and of infinite horizontal extent. The fluid is Newtonian, and we apply the Boussinesq approximation. The wall $z = 0$ is maintained at a temperature $T_0 + \Delta T$, with the upper wall at a temperature T_0. We introduce non-dimensional variables, scaling length, time, velocity, pressure and temperature according to $d, d^2\kappa, (\alpha g\kappa\Delta T d\nu^{-1})^{\frac{1}{2}}, (\rho_0^2\kappa\alpha g\nu\Delta T d^{-1})^{\frac{1}{2}}$, and ΔT respectively. The governing equations are then as follows,

$$\sigma^{-1}\left(\mathbf{v}_t + R^{\frac{1}{2}}\mathbf{v}\cdot\nabla\mathbf{v}\right) = \nabla^2\mathbf{v} - \nabla p + R^{\frac{1}{2}}T\hat{\mathbf{k}}, \tag{2.1a}$$

$$\nabla\cdot\mathbf{v} = 0, \tag{2.1b}$$

$$T_t + R^{\frac{1}{2}}\mathbf{v}\cdot\nabla T = \nabla^2 T, \tag{2.1c}$$

where, $\sigma = \nu/\kappa$, is the Prandtl number and $R = \alpha g\Delta T d^3/\kappa\nu$ is the Rayleigh number. In the above, subscripts denote partial differentiation, and the operator ∇^2 is defined as,

$$\nabla^2 = \frac{\partial^2}{\partial x^2} + \frac{\partial^2}{\partial y^2} + \frac{\partial^2}{\partial z^2}$$

The velocity, pressure and temperature fields are denoted by the quantities, $\mathbf{v} = (u, v, w)$, P and T respectively, whilst $\hat{\mathbf{k}}$, represents the unit vector in the positive z direction. Also, ρ_0, ν, κ and α, are typical values for the density, kinematic viscosity, thermal diffusivity and coefficient of thermal expansion respectively.

Before proceeding, we first describe the feedback control mechanism introduced by Tang and Bau (1993). It consists of sensors placed at some horizontal cross-section, in our case, the midlayer, and actuators on the lower surface, which react to any deviation of the fluid temperature from the desired conductive values by modifying the temperature distribution there, and thus, increasing the dissipation of these disturbances.

The no-motion state of the classical problem is a solution of the equations of motion for all values of the Rayleigh number . However, as a result of imperfections within the system, the temperature field may deviate from its conductive value, and thus buoyant forces are produced, inducing fluid motion. Below the critical Rayleigh number for the classical problem, thermal conduction is sufficient to dissipate these disturbances and

hence, the no-motion state is restored. The controller introduced, may assist in this dissipation, and thus the critical value of the Rayleigh number maybe be increased.

We assume that the temperature distribution at $z = \frac{1}{2}$, is known, or maybe calculated to sufficient accuracy and is a continuous function of (x, y). In the no-motion state,

$$T_{z=0} = 0.$$

Given some deviation from the initial distribution, the actuators modify the lower surface temperature according to,

$$T_{z=0} = \hat{K}_p \overline{T} + \hat{K}_n \overline{T}^2, \tag{2.2}$$

where $\overline{T} = T(z = \frac{1}{2})$ and $\hat{K}_p$ and $\hat{K}_n$ are the gains of proportional and nonlinear controllers respectively.

Once the disturbance has been dissipated, $T_{z=0}$ again takes its initial value of zero. In normal operating conditions, the controller reacts before the disturbance has a chance to grow, and any deviation in the lower surface temperature will be small. Thus we make the assumption that the control parameters, $\hat{K}_p$ and $\hat{K}_n$ are small, and thus introduce,

$$\hat{K}_p = K_p \delta, \qquad \hat{K}_n = K_n \delta,$$

where, δ is a small parameter, and K_p, and K_n are both $O(1)$ quantities.

The walls at $z = 0$ and $z = 1$ are taken to be planar, stress-free surfaces, and conditions of no slip and zero stress are imposed, together with the assumption that the boundaries are isothermal. These conditions may be re-written in terms of the temperature variable as,
On $z = 0$,

$$T = K_p \overline{T} \delta + K_n \overline{T}^2 \delta, \tag{2.3a}$$

$$\nabla^2 T = \nabla^4 T = 0 \tag{2.3b}$$

and on $z = 1$,

$$T = \nabla^2 T = \nabla^4 T = 0 \tag{2.4}$$

Again, $\overline{T}$, is defined as the temperature on the surface, $z = \frac{1}{2}$.

We note that boundary conditions for T are,

$$D^2 T = D^4 T = 0, \text{ on } z = 0, 1$$

together with suitable conditions on T at the upper and lower surfaces. However, due to the control mechanism under investigation, these conditions depend on δ. In the above, D denotes partial differentiation with respect to z.

We wish to concentrate on the nonlinear evolution of interacting modes, and we seek solutions with R differing from its critical value by $O(\epsilon^2)$, where ϵ is considered to be small. We therefore expand R as,

$$R = R_0 + \hat{\epsilon}^2 R_2 + \ldots. \tag{2.5}$$

Note that in the above, R_0 and R_2, are dependent on δ, and in addition, we scale the time dependence such that $t = \hat{\epsilon}^2\tau$, where τ is an $O(1)$ quantity.

Here, we wish to concentrate on the roll of feedback control on the pattern selection problem in the weakly nonlinear regime, and apply the results of previous authors (see Segel and Stuart 1962, Segel 1965) for the slightly non-Boussinesq fluid to aid in interpreting our results. The latter authors considered pattern selection involving rolls and hexagons, and found that the problem reduces to the investigation of the non-linear interactions of a triad of modes with wave-numbers,

$$(k_x, k_y) = \frac{\pi}{\sqrt{2}}\left(\frac{1}{2}, \frac{-\sqrt{3}}{2}\right), \tag{2.6a}$$

$$(k_x, k_y) = \frac{\pi}{\sqrt{2}}\left(\frac{1}{2}, \frac{+\sqrt{3}}{2}\right), \tag{2.6b}$$

$$(k_x, k_y) = \frac{\pi}{\sqrt{2}}(1, 0). \tag{2.6c}$$

In the absence of the controller, we expand the temperature perturbation as,

$$T = 1 - z + \hat{\epsilon}\sin\pi z\,(XE_1 + YE_2 + ZE_3) + c.c. + \ldots, \tag{2.7}$$

where,

$$E_1 = \exp\frac{i\pi}{\sqrt{2}}\left(\frac{x}{2} - \frac{\sqrt{3}}{2}y\right), \tag{2.8a}$$

$$E_2 = \exp\frac{i\pi}{\sqrt{2}}\left(\frac{x}{2} + \frac{\sqrt{3}}{2}y\right), \tag{2.8b}$$

$$E_3 = \exp\frac{i\pi}{\sqrt{2}}x, \tag{2.8c}$$

and X, Y and Z, are functions of time only whilst *c.c.* denotes the complex conjugate.

If the non-Boussinesq effects are taken to be small, $O(\hat{\epsilon})$, then the amplitude equations for X, Y and Z, are of a similar form to those of Segel and Stuart (1962), where variation of the fluid properties with temperature is taken into account. However, since we assume that viscosity is constant, the quadratic term in these equations vanish. We leave the discussion of this system of equations until the following section.

In order to determine the effects of feedback control upon pattern selection development, we shall expand the temperature and velocity fields as follows,

$$T = T_B + \hat{\epsilon}T_1 + \hat{\epsilon}^2T_2 + \ldots, \tag{2.9a}$$

$$\mathbf{v} = \hat{\epsilon}\mathbf{v}_1 + \hat{\epsilon}^2\mathbf{v}_2 + \ldots. \tag{2.9b}$$

We now substitute the above into the governing equations (2.1a-c) and equating like powers of $\hat{\epsilon}$ and then δ we obtain a solution in the following manner.

In the basic state, the fluid is at rest. The temperature field, $T_B(z)$, and Rayleigh number R_0 are expanded below,

$$T_B = T_{B0} + \delta T_{B1} + \delta^2 T_{B2} + \ldots, \tag{2.10a}$$
$$R_0 = R_{00} + \delta R_{01} + \ldots, \tag{2.10b}$$

where,

$$T_{B0} = 1 - z \tag{2.11}$$

and

$$T_{B1} = \gamma_1 (1 - z), \tag{2.12a}$$
$$\gamma_1 = K_p \overline{T}_{B0} + K_n \overline{T}_{B0}^2. \tag{2.12b}$$

Similarly,

$$T_{B2} = \gamma_2 (1 - z), \tag{2.13a}$$
$$\gamma_2 = K_p \overline{T}_{B1} + 2K_n \overline{T}_{B0} \overline{T}_{B1}. \tag{2.13b}$$

At $O(\hat{\epsilon})$, we again expand the temperature and velocity perturbations in powers of δ,

$$T_1 = T_{10} + \delta T_{11} + \ldots \tag{2.14a}$$
$$\mathbf{v}_1 = \mathbf{v}_{10} + \delta \mathbf{v}_{11} + \ldots \tag{2.14b}$$

The problem for T_{10} reduces to,

$$-\nabla^6 T_{10} + R_{00} \nabla_1^2 T_{10} = 0, \tag{2.15}$$

where

$$\nabla_1^2 = \frac{\partial^2}{\partial x^2} + \frac{\partial^2}{\partial y^2},$$

with the boundary conditions:

$$T_{10}(0) = D^2 T_{10}(0) = D^4 T_{10}(0) = 0, \tag{2.16a}$$
$$T_{10}(1) = D^2 T_{10}(1) = D^4 T_{10}(1) = 0. \tag{2.16b}$$

The solution to the above maybe written as,

$$T_{10} = \phi \sin \pi z \tag{2.17}$$

where,

$$\nabla_1^2 \phi + \frac{\pi^2}{2} \phi = 0, \tag{2.18a}$$
$$\phi = X(t) E_1 + Y(t) E_2 + Z(t) E_3 + c.c., \tag{2.18b}$$

where, E_1, E_2 and E_3 are as previously defined in (2.8a-c). In this way we find the critical Rayleigh number , R_{00} to be equal to $27\pi^4/4$.

Again at $O(\hat{\epsilon}^2)$, we expand T_2 and $\mathbf{v}_2$, as power series in δ, as in (2.14a,b), and find that the leading order problem for T_{20} and $\mathbf{v}_{20}$ has a solution given by,

$$T_{20} = \sum_{m=0,4} L_m \Phi_m \sin 2\pi z, \tag{2.19a}$$

$$w_{20} = \sum_{m=0,4} P_m \Phi_m \sin 2\pi z, \tag{2.19b}$$

$$\begin{pmatrix} u_{20} \\ v_{20} \end{pmatrix} = \sum_{m=0,4} Q_m \begin{pmatrix} \Phi_{mx} \\ \Phi_{my} \end{pmatrix} \cos 2\pi z. \tag{2.19c}$$

In the above, L_m, P_m and Q_m are constants, determined from the system of equations governing this order and the subscripts, x and y denotes partial differentiation with respect to the x and y co-ordinates respectively. The functions Φ_m are given by,

$$\Phi_0 = 2\left(|X|^2 + |Y|^2 + |Z|^2\right), \tag{2.20a}$$

$$\Phi_1 = 2\overline{Y}ZE_1 + 2\overline{X}ZE_2 + 2XYE_3 + c.c, \tag{2.20b}$$

$$\Phi_2 = 0, \tag{2.20c}$$

$$\Phi_3 = 2X\overline{Y}E_1\overline{E_2} + 2XZE_1E_3 + 2YZE_2E_3 + c.c, \tag{2.20d}$$

$$\Phi_4 = X^2E_1^2 + Y^2E_2^2 + Z^2E_3^2 + c.c, \tag{2.20e}$$

and thus,

$$\nabla_1^2 \Phi_m = -m\frac{\pi^2}{2}\Phi_m.$$

We note that this solution satisfies homogeneous boundary conditions on the temperature at the lower surface.

At $O(\hat{\epsilon}\delta)$, we find that T_{11} satisfies,

$$-\nabla^6 T_{11} + R_{00}\nabla_1^2 T_{11} = -\left(R_{00}\gamma_1 + R_{01}\right)\nabla_1^2 T_{10}, \tag{2.21a}$$

$$T_{11}(0) = (K_p + K_n)\,\phi, \tag{2.21b}$$

$$T_{11}(1) = \nabla^2 T_{11}(0) = \nabla^2 T_{11}(1) = \nabla^4 T_{11}(0) = \nabla^4 T_{11}(1) = 0, \tag{2.20d}$$

with solution,

$$T_{11} = \phi\hat{T}(z), \tag{2.21a}$$

$$\hat{T}(z) = A_T(z-1)\cos\pi z + \sum_{j=1,4} B_j \exp\lambda_j z, \tag{2.21b}$$

where A_T is a constant given by,

$$A_T = \frac{R_{00}\gamma_1 + R_{01}}{27\pi^3}, \tag{2.22}$$

and λ_j are roots to the equation,

$$\left(\lambda_j^2 - \frac{\pi^2}{2}\right)^3 + R_{00}\frac{\pi^2}{2} = 0,$$

other than $\pm i\pi$. Values for A_T, and B_j in (2.21a) are found from the boundary conditions, which reduce to solving a matrix equation of the form,

$$\mathbf{P}\mathbf{x} = (K_p + K_n)\,\mathbf{Q}. \tag{2.23}$$

Hence, from (2.22), a value for R_{01} may also be determined.

Since we wish to consider the evolution of the amplitudes, X, Y and Z, at $O(\hat{\epsilon}^3)$, and include nonlinear effects from both the controller and terms in the governing equations, we require that $\hat{\epsilon}$ and δ are of comparable orders of magnitude. Thus, we shall combine the solutions to the problems at $O(\hat{\epsilon}^3), O(\hat{\epsilon}^2\delta)$ and $O(\hat{\epsilon}\delta^2)$. In other words we now set

$$\hat{\epsilon} = \delta.$$

At this order, the solvability condition required for a solution of the differential system to exist yields the following equations for the amplitudes X, Y and Z,

$$\Sigma\dot{X} = (\epsilon+\alpha)\,X - a\overline{Y}Z - X\left(R_1 \mid X \mid^2 + P \mid Y \mid^2 + P \mid Z \mid^2\right) \tag{2.24a}$$

$$\Sigma\dot{Y} = (\epsilon+\alpha)\,Y - a\overline{X}Z - Y\left(R_1 \mid Y \mid^2 + P \mid X \mid^2 + P \mid Z \mid^2\right) \tag{2.24b}$$

$$\Sigma\dot{Z} = (\epsilon+\alpha)\,Z - aXY - Z\left(R_1 \mid Z \mid^2 + P \mid X \mid^2 + P \mid Y \mid^2\right) \tag{2.24c}$$

In the above, a and α are functions of the control parameters K_p and K_n and given by,

$$\begin{aligned}\alpha &= \pi^2\left(\gamma_1 R_{00} + R_{01}\right)\left(-\frac{A_T}{4\pi}\sum_{j=1,4} B_j\pi\frac{e^{\lambda_j}+1}{\lambda_j^2+\pi^2}\right) \qquad (2.25a)\\ &+ \frac{\pi^2}{2}\left(\gamma_1 R_{01} + \gamma_2 R_{00}\right) + \frac{9\pi^5}{2}\left(K_p\hat{T}_{11}\left(\frac{1}{2}\right) + K_n\left(\hat{T}_{11}\left(\frac{1}{2}\right) + \gamma_1\right)\right),\\ a &= 9\frac{\pi^3}{2}\left[-\pi A_T + \sum_{j=1,4}\left(\frac{\pi^2}{2} - \lambda_j^2\right)B_j\frac{2\pi\left(1-e^{\lambda_j}\right)}{\lambda_j^2+\pi^2}\right] \qquad (2.25b)\\ &+ 2R_{00}^{\frac{1}{2}}\left[-3\pi^2\hat{T}(0) - \frac{81\pi^7}{16R_{00}^{\frac{1}{2}}}\left(-\frac{2A_T}{3\pi} + \sum_{j=1,4}B_j\frac{2\pi\left(1-e^{\lambda_j}\right)}{\lambda_j^2+\pi^2}\right)\right]\\ &- 9\pi^5 K_n.\end{aligned}$$

We note that from, (2.23), the constants, A_T, and B_j, are proportional to $K_p + K_n$. From this, and the above expression for a, we obtain the following, simplified expression for the dependence of a on the control parameters, K_p and K_n,

$$a = a_1\left(K_p + K_n\right) + a_2 K_n, \tag{2.26}$$

where a_1 and a_2 are constants.

In addition,

$$\Sigma = \frac{9\pi^4}{4}\left(1+\frac{1}{\sigma}\right),$$

and,

$$\epsilon = \frac{\pi^2}{2}\left(R_{20}+R_{11}+R_{02}\right).$$

and R_1 and P are constants.

3 Solution of the amplitude equation

We seek steady solutions of (2.24a-c) with,

$$X = x_0 \tag{3.1a}$$
$$Y = y_0 \tag{3.1b}$$
$$Z = z_0. \tag{3.1c}$$

In the above, x_0, y_0 and z_0, are constants satisfying the following system of equations,

$$0 = (\epsilon+\alpha)\,x_0 - a\overline{y_0}z_0 - x_0\left(R_1 \mid x_0 \mid^2 + P \mid y_0 \mid^2 + P \mid z_0 \mid^2\right) \tag{3.2a}$$
$$0 = (\epsilon+\alpha)\,y_0 - a\overline{x_0}z_0 - y_0\left(R_1 \mid y_0 \mid^2 + P \mid x_0 \mid^2 + P \mid z_0 \mid^2\right) \tag{3.2b}$$
$$0 = (\epsilon+\alpha)\,z_0 - ax_0y_0 - z_0\left(R_1 \mid z_0 \mid^2 + P \mid x_0 \mid^2 + P \mid y_0 \mid^2\right) \tag{3.2c}$$

With the control switched off, $K_p = K_n = 0$, we note that α and a are both zero, and from Segel and Stuart (1962), and Segel (1965), possible equilibrium solutions are,

$$\text{I Conduction} \;:\; x_0 = y_0 = z_0 = 0, \tag{3.3a}$$
$$\text{IIa,b Rolls} \;:\; x_0 = y_0 = 0, z_0 = \pm\left(\frac{\epsilon}{R_1}\right)^{\frac{1}{2}}, \tag{3.3b}$$
$$\text{IIIa,b Hexagons} \;:\; x_0 = y_0 = z_0, z_0 = \mp(2T)^{-1}\sqrt{4\epsilon T}, \tag{3.3c}$$
$$\text{IVa,b Hexagons} \;:\; x_0 = y_0 = -z_0, z_0 = \mp(2T)^{-1}\sqrt{4\epsilon T}, \tag{3.3d}$$
$$\text{V Mixed} \;:\; z_0 = 0, x_0 = y_0 = \pm\sqrt{R\epsilon}, \tag{3.3e}$$

where $Q = P - R_1, 4R = P + R_1$ and $T = P + 4R$.

The stability of the different solutions may be found by an examination of the linear growth rates of small perturbations to x_0, y_0 and z_0 as discussed in appendix 4 of Segel (1965). The equilibrium forms for z_0 given by (3.3a,e), are shown in figure 1, with the Prandtl number set to unity. Unstable solutions are represented by dashed curves.

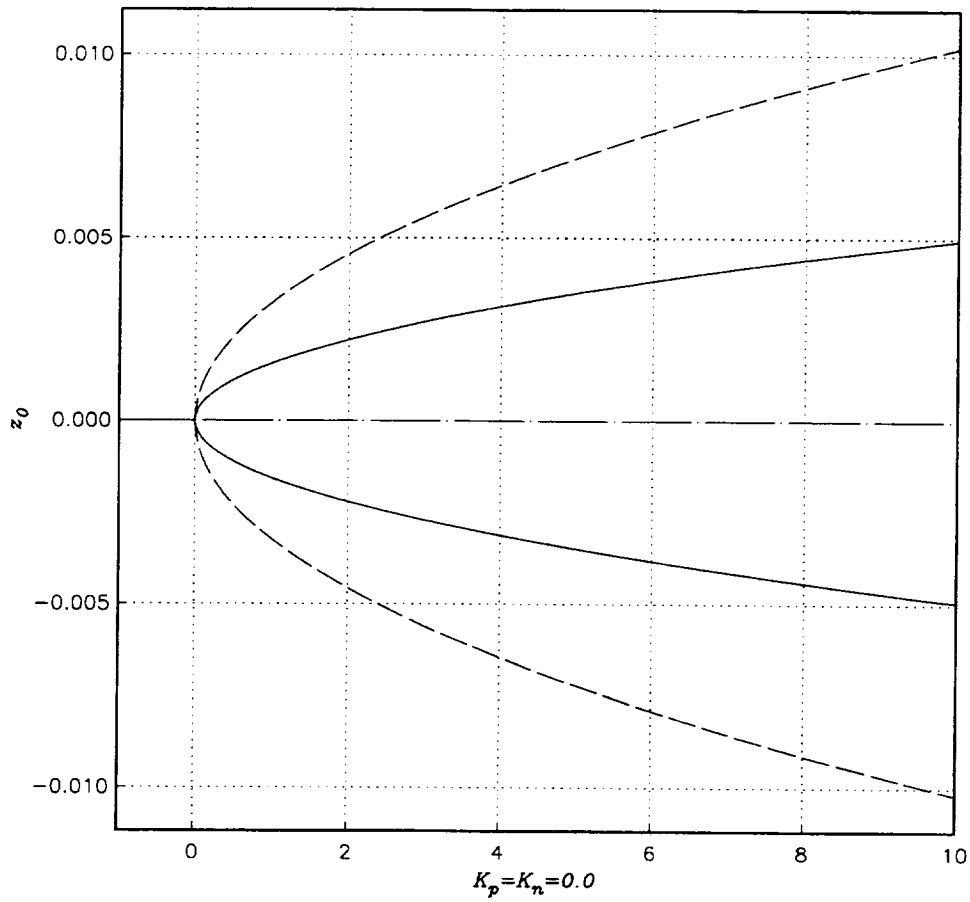

Figure 1: Equilibrium forms for z_0, given by (3.3a,e)

We now go on to describe how the bifurcation picture is modified by the effects of feedback control on the system. We first write down the equilibrium solutions satisfied by the controlled problem,

$$\text{I Conduction} \quad : \quad x_0 = y_0 = z_0 = 0, \tag{3.4a}$$

$$\text{IIa,b Rolls} \quad : \quad x_0 = y_0 = 0, z_0 = \pm\left(\frac{\epsilon+\alpha}{R_1}\right)^{\frac{1}{2}}, \tag{3.4b}$$

$$\text{IIIa,b Hexagons} \quad : \quad x_0 = y_0 = z_0, z_0 = (2T)^{-1}\left(-a \mp \sqrt{a^2+4T(\epsilon+\alpha)}\right), \tag{3.4c}$$

$$\text{IVa,b Hexagons} \quad : \quad x_0 = y_0 = -z_0, z_0 = (2T)^{-1}\left(-a \mp \sqrt{a^2+4T(\epsilon+\alpha)}\right), \tag{3.4d}$$

$$\text{V Mixed} \quad : \quad z_0 = \frac{-a}{Q}, x_0 = y_0 = \pm R^{\frac{1}{2}}\left(\epsilon+\alpha-\frac{R_1 a^2}{Q^2}\right)^{\frac{1}{2}}, \tag{3.4e}$$

where Q, P, R_1, R and T are as previously defined.

Clearly, for solutions of types II-V to exist, ϵ must be greater than some threshold value given by,

$$\text{III, IV} \quad : \quad \epsilon = B1 = \frac{a^2}{4T} - \alpha, \tag{3.5a}$$

$$\text{II} \quad : \quad \epsilon = B2 = -\alpha, \tag{3.5b}$$

$$\text{V} \quad : \quad \epsilon = A1 = \frac{R_1 a^2}{Q^2} - \alpha. \tag{3.5c}$$

In addition, it can be shown by a linear stability analysis, that the hexagonal cell pattern loses stability at,

$$\epsilon = A2 = \frac{R_1 a^2}{Q^2} - \alpha. \tag{3.6}$$

The first point to note is that a subcritical bifurcation to the hexagonal cell pattern remains viable. This is due to the fact that all three modes will have the same critical values of ϵ, corresponding to linear instability, since the control mechanism has no preferred direction, unlike say the shear flow mechanisms discussed by Hall and Kelly, where the effect of the shear is felt only by modes not aligned parallel to the shear.

We now go on to examine the case where only the proportional controller, K_p, is in operation, and see how the bifurcation diagram changes.

Figure 2 illustrates how the bifurcation picture is modified for $K_p = \pm 0.02$. Again, the stability of the solutions can be found by an examination of a linearised analysis of the growth rates of small perturbations to the equilibrium solutions. For $K_p < 0$, the parameter a in equations (3.4a-c) is positive and from Segel and Stuart (1962), we deduce that the zero amplitude solution, I, loses stability at $\epsilon = \alpha$ corresponding to B2, so that a hexagonal pattern corresponding to either IIIa or IVa will be generated as ϵ is increased further. This mode however is destabilised at A2.

This loss in stability is due to the effects of the mixed mode V, which is unstable for all values of ϵ, and originates as a bifurcation from the roll mode IIb at A1. Beyond A1, IIb becomes stable, and thus as the Rayleigh number is further increased, the hexagonal cells are replaced by the rolls corresponding to this solution. If the Rayleigh number is subsequently decreased, hysteresis can occur with the roll pattern persisting until A1 at which point the hexagonal cells are re-established.

For $K_p > 0$, a similar scenario occurs. However, the parameter a is, in this case negative and thus instead of hexagonal cells corresponding to the equilibrium solutions IIIa or IVa being established at $B2$, the cell patterns IIIb or IVb are initially generated. In addition the mixed mode bifurcates from rolls of type IIa, and it is this mode which becomes the stable solution beyond A1, with the roll pattern established at A2.

In addition, it should be noted that the roll mode solutions cannot exist until $\epsilon = -\alpha$, and for all values of K_p, α is positive. This implies that the initial destabilisation of the

conduction mode, I, and transition to the hexagonal cells, occurs for values of ϵ in excess of $\epsilon = 0$, the critical value of the uncontrolled problem. However, the hexagonal type solutions III, and IV, become viable solutions for $\epsilon < 0$ for all $K_p \neq 0$, and thus if the Rayleigh number were decreased, hysteresis effects occur for subcritical values of ϵ, that is, the closed cell pattern persists for negative values of this parameter. Figures 4 and 5 describe how the location of the points $B1$, $B2$ and $A1$, $A2$, vary with K_p and illustrates the points discussed above.

The stability of the various modes for $K_p > 0$ and $K_p < 0$ are outlined below.

	$K_p < 0$		$K_p > 0$	
I	Stable until	$\epsilon \geq -\alpha$	Stable until	$\epsilon \geq -\alpha$
IIa	Unstable for all ϵ		Stable for	$\epsilon \geq A1$
IIb	Stable for	$\epsilon \geq A1$	Unstable for all ϵ	
IIIa, IVa	Stable for	$B1 \leq \epsilon \leq A2$	Unstable for all ϵ	
IIIb, IVb	Unstable for all ϵ		Stable for	$B1 \leq \epsilon \leq A2$
V	Unstable for all ϵ		Unstable for all ϵ	

Figure 3, shows how the bifurcation picture develops for larger values of $\mid K_p \mid$. As this parameter is increase, $B1 \rightarrow -\infty$ and $B2 \rightarrow +\infty$, and thus the no-motion state remains stable for longer. In addition, subsequent destabilisation of the hexagonal pattern is also delayed, that us, the range of ϵ over which solutions III or IV are stable increases with K_p.

We next consider the effects of the nonlinear controller on the bifurcation diagram, with the proportional controller, K_p, set to zero.

In figure 6, we show the bifurcation diagrams for small values of the nonlinear controller, $K_n = \pm 0.02$. As in the previous case, stability of the various solutions depends on the sign of a in equations (3.4a). For, $K_n > 0$, a is negative and vice versa. Thus the stable/unstable modes are as previously discussed and outlined in Segel (1965). Again, after the loss of stability of the conduction mode I, an hexagonal cell pattern corresponding to either solution III or IV, is initially established. Due to the mixed mode V, these modes loses stability at $A2$, and transition to the stable roll pattern II occurs as ϵ is increased. If the Rayleigh number is then decreased hysteresis occurs, with the hexagonal mode not being re-established until $A1$.

One important feature to be considered in this case is that both the roll and hexagonal modes become viable solutions for $\epsilon < 0$. Thus the initial transition from the no-motion state to the closed cells of solutions III and IV, occurs as a subcritical bifurcation. In figure 8 where we plot $B1$ and $B2$, the thresholds above which solutions III,IV and II may exist respectively, against K_n. As can be seen for all K_n, these threshold values are negative, and thus transition from the no-motion state occurs for subcritical values of ϵ. In addition, we see from figure 9, that $A1$ and $A2$, the positions where the roll mode

becomes stable and destabilisation of the hexagonal cells occur respectively, occur for positive ϵ.

Finally let us look at the case where both controllers are in operation. Figure 10, illustrates the change in behaviour of the points $B1$ and $B2$, which represent the values of ϵ above which solutions III, IV and II exist respectively. We recall that for $K_n = 0$, for all K_p, $B1 < 0$ and $B2 > 0$, and for $K_p = 0$, for any value of K_n, $B1, B2$ were both negative. An important feature shown in figure 10 is that this behaviour can be modified such that there now exists a range of values of K_p for a given K_n, for which $B1 > 0$, that is to say the hexagonal cell pattern is not a viable solution until above $\epsilon = 0$, the critical value of the uncontrolled problem. In this case K_n was varied between 0.0, and 0.2 . Negative values of this parameter give similar plots, reflected in the line $K_p = 0.0$.

In addition, by careful choice of K_p for a given K_n, it is possible to create scenarios with,

$$B1 < 0, \quad B2 < 0, \qquad B1 < 0, \quad B2 > 0, \qquad B1 > 0, \quad B2 > 0.$$

Since $B1 \leq B2$ for all K_p, K_n, it is not possible to generate the case where, $B1 > 0, B2 < 0$.

The bifurcation diagrams for these different cases are shown in figure 11. Here, solid lines represent stable solutions to the problem, whilst the dashed lines are unstable. In addition, we note that for the values in the parameters considered, except for certain cases, the solution corresponding to the mixed mode does not show up in these diagrams. This is due to the fact that the bifurcation from which this mode originates occurs for large values of ϵ, out of the range illustrated here. However, behaviour will be similar to that discussed above, with the mixed mode originating as a bifurcation from the roll modes, at $\epsilon = A1$. Above this value, the roll mode solution will be stable, and the hexagonal cell structure will subsequently be destabilised due to interaction with the mixed modes, at $A2$. For larger ϵ, either IIa or IIb provides a stable equilibrium solution to the equations of motion.

For $K_p = -0.55, K_n = +0.05$, we see that the hexagonal cell pattern becomes viable for $\epsilon < B1 < 0$, whilst the roll modes cannot occur until $\epsilon > B2 > 0$. This is due to the fact that the linear controller dominates over the nonlinear controller K_n, and thus we see behaviour typical of the $K_n = 0, K_p \neq 0$ discussed previously.

As K_p is increased $B1$ moves through the origin, and solutions III and IV occur for positive value of ϵ, whilst $B2$, moves towards $\epsilon = 0$. This behaviour is due to the relative dependence of the parameters α and a on K_p and K_n. For this parameter range, some cancellation of the effects of each controller on α and a is occurring leading to supercritical behaviour, that is to say that the destabilisation of the no-motion state I, occurs for values of ϵ in excess of the critical value of the uncontrolled problem. These points eventually coalesce and this case, being of some interest, is discussed later.

For further increases in K_p, $B1$ again becomes negative and, for even larger K_p the roll solutions II also become viable for $\epsilon < 0$, and thus the initial bifurcation form the conductive state to the hexagonal cell pattern is subcritical in nature. Within this

parameter range, the nonlinear controller dominates the regulation of the lower surface temperature. $B2$ again becomes positive for larger values of K_p, with $B1$ remaining negative in value. Here the relative effects of the controllers are such that the linear controller again dominates.

The stability characteristics for each of these cases are as previously discussed. The no-motion state loses stability at $\epsilon = -\alpha$, corresponding to point $B2$, and the hexagonal cell pattern, forms as the stable solution. Due to the influence of the mixed mode V, which results as a bifurcation from the roll modes, this pattern is then destabilised at $A2$, and rolls are formed. Subsequent decreases in the Rayleigh number lead to hysteresis effects, with the roll modes persisting until $A1$, at which point the hexagonal cells are re-established.

As mentioned previously, points $B1$ and $B2$ can coalesce. From the form of the equilibrium solutions given in (3.4a-e), we can see that this occurs when $a = 0$. Due to the dependence of a on K_p and K_n, given by, (2.26), a relationship between the control parameters maybe written down,

$$K_p = -\frac{a_1 + a_2}{a_1} K_n, \tag{3.7}$$

where a_1 and a_2 are constants. In addition at this point, the equilibrium solutions reduce to,

$$\text{I Conduction} \quad : \quad x_0 = y_0 = z_0 = 0, \tag{3.8a}$$

$$\text{IIa,b Rolls} \quad : \quad x_0 = y_0 = 0, z_0 = \pm \left(\frac{\epsilon + \alpha}{R_1}\right)^{\frac{1}{2}}, \tag{3.8b}$$

$$\text{IIIa,b Hexagons} \quad : \quad x_0 = y_0 = z_0, z_0 = \mp (2T)^{-1} \sqrt{4(\epsilon + \alpha) T}, \tag{3.8c}$$

$$\text{IVa,b Hexagons} \quad : \quad x_0 = y_0 = -z_0, z_0 = \mp (2T)^{-1} \sqrt{4(\epsilon + \alpha) T}, \tag{3.8d}$$

$$\text{V Mixed} \quad : \quad z_0 = 0, x_0 = y_0 = \pm \sqrt{R(\epsilon + \alpha)}. \tag{3.8e}$$

A typical bifurcation diagram for K_n and K_p satisfying (3.7), is shown in figure 12. Here, solutions corresponding to IIa,b are shown as dotted lines, whilst the hexagonal cell patterns IIIa,b and IVa,b are solid. As can be seen, the picture is very similar to that for the equilibrium solutions for z_0 with no control, (figure 1), except that the bifurcation from the no-motion state occurs for $\epsilon = -\alpha$. The roll and hexagonal modes become possible solutions to the equations of motion at this point, as indeed does the mixed mode, which corresponds to a solution with no-motion in the z-direction. Beyond $\epsilon = \alpha$, the conduction mode, loses stability, and the hexagonal cell pattern is formed. Since the mixed mode V originates as a bifurcation from the roll solutions II at the same point, $\epsilon = \alpha$, and no interaction between this mode and modes III or IV is possible, there can be no subsequent transition from the hexagonal cells to rolls . In addition, if the Rayleigh number were decreased from above $\epsilon = -\alpha$, no hysteresis effects are seen.

4 Further comments and conclusions

We have given a description of the process by which a control strategy maybe used to delay or indeed speed up the onset of convection in a Boussinesq fluid. The amplitude equations derived describe the effects of both linear and nonlinear proportional controllers on the flow regime.

Since the controller has no preferred direction, a subcritical bifurcation to the hexagonal cell pattern remains viable. We considered three cases in detail. Firstly, with only the linear controller in operation, we found that the onset of convective instabilities was delayed, and that the hexagonal cell pattern persists for longer as the control parameter K_p is increased. If the linear controller is switched off, and thus the lower surface temperature is only regulated by the nonlinear controller, the transition from the no-motion state to a hexagonal cell pattern occurs for subcritical values of the Rayleigh number. The most interesting case was with both controllers in operation. Here, a range of different behaviours is possible. In particular the exists a parameter range for which the hexagonal cell patterns do not become viable solutions to the model for values of ϵ greater than zero. Thus, not only is the onset of convection delayed significantly, but hysteresis effects would lead to the re-establishment of the no-motion state for values of ϵ in excess of the critical value for the uncontrolled problem. In addition, for a given value of the parameter K_n, we have shown that there exists a K_p such that the onset of convection is supercritical, and the solutions corresponding to the roll, hexagonal and mixed modes all bifurcate from the same point, thus the hexagonal cell pattern remains the stable solution for Rayleigh numbers in excess of this point.

To conclude, careful choice of the various parameters involved, can either delay the onset of convection, or produce transition for subcritical values of the Rayleigh number.

References

[1] Busse, F.H. 1967, Nonstationary finite amplitude convection.
J. Fluid Mechanics **28**, 223-239.

[2] Davis, S.H. 1976, The stability of time-periodic flows.
A. Rev. Fluid Mech. **8**, 57-74.

[3] Donnelly, R.J. 1990, Externally modulated hydrodynamic systems.
Nonlinear evolution of Spatio-Temporal structures in Dissipative Continuous Systems
ed. F.H. Busse and L. Kramer
pp. 31-43. Plenum.

[4] Hall, P. 1995, Finite amplitude convection in the presence of an unsteady shear flow.
J. Fluid Mechanics **287**, 225-249.

[5] Hall, P. and Kelly, R.E. 1995, On the effect of a shear flow on the planform of thermal convection in a fluid of variable viscosity.
Phys. Rev. E **52**, 3687-3696.

[6] Kelly, R.E. 1993, The onset and development of thermal convection in fully developed shear flows.
Advances in Applied Mechanics, **30**.

[7] Kelly, R.E. and Hu, H.C. 1993, The onset of Rayleigh-Bénard convection in non-planar oscillatory flows.
J. Fluid Mechanics **249**, 373-390.

[8] Meyer, C.W., Cannel, D.S. and Ahlers, G. 1992, Hexagonal and roll flow patterns in temporally modulated Rayleigh-Bénard convection.
Phys. Rev. A **45**, 8583-8604.

[9] Palm, E., Ellingsen, T. and Gjevik, V. 1967, On the occurrence of cellular motion in Bénard convection.
J. Fluid Mechanics **30**, 651-661.

[10] Roppo, M.N., Davis, S.H. and Rosenblat, S. 1984, Bénard Convection with time-periodic heating.
Phys. Fluids **27**, 796-803.

[11] Segel, L.A. 1965, On the occurrence of cellular motion in Bénard convection.
J. Fluid Mechanics **21**, 359-384

[12] Segel, L.A. and Stuart, J.T. 1962, On the preferred mode in cellular thermal convection.
J. Fluid Mechanics **13**, 289-306

[13] Singer, J. and Bau, H.H. 1991, Active control of convection.
Phys. Fluids A **3**, 2859-2865.

[14] Singer, J., Wang, Y.Z., Bau, H.H. 1991, Controlling a chaotic system.
Phys. Rev. Lett. **66**, 1123-1125.

[15] Tang, J. and Bau, H.H. 1993, Feedback control stabilisation of the no-motion state of a fluid confined in a horizontal porous layer heated from below.
J. Fluid Mechanics **257**, 485-505.

[16] Tang, J. and Bau, H.H. 1993, Stabilisation of the no-motion state in Rayleigh-Bénard convection through the use of feedback control.
Phys. Rev. Lett. **70**, 1755-1798.

[17] Wang, Y.Z., Singer, J. and Bau, H.H. 1992, Controlling chaos in a thermal convection loop.
J. Fluid Mechanics **237**, 479-498.

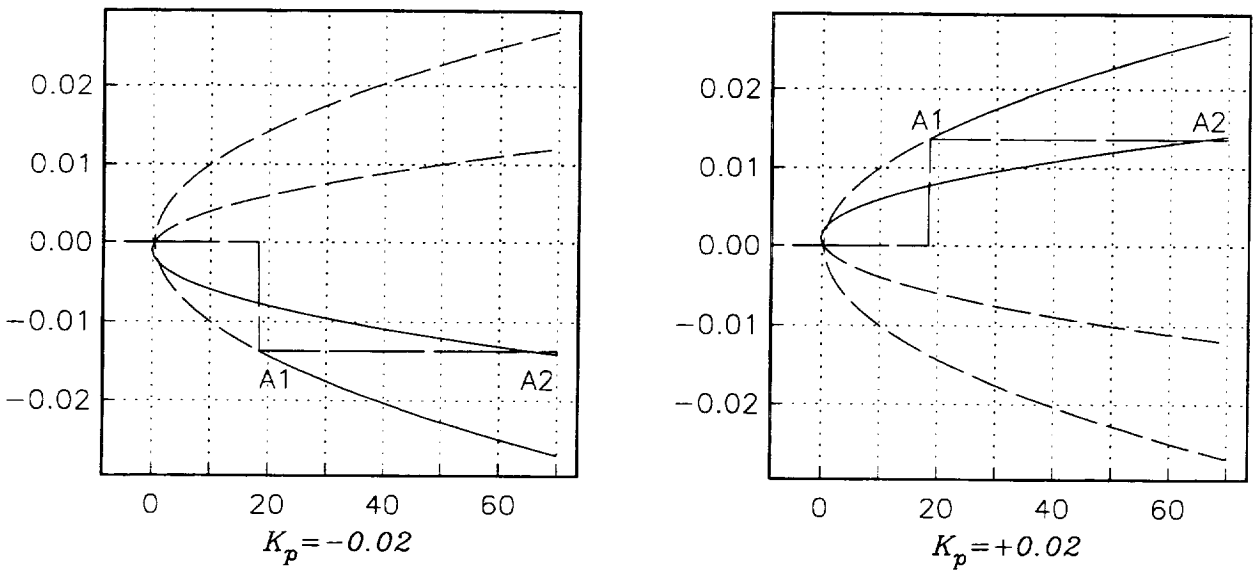

Figure 2: Z_0 vs ϵ for $K_p = \pm 0.02$, K_n=0.0

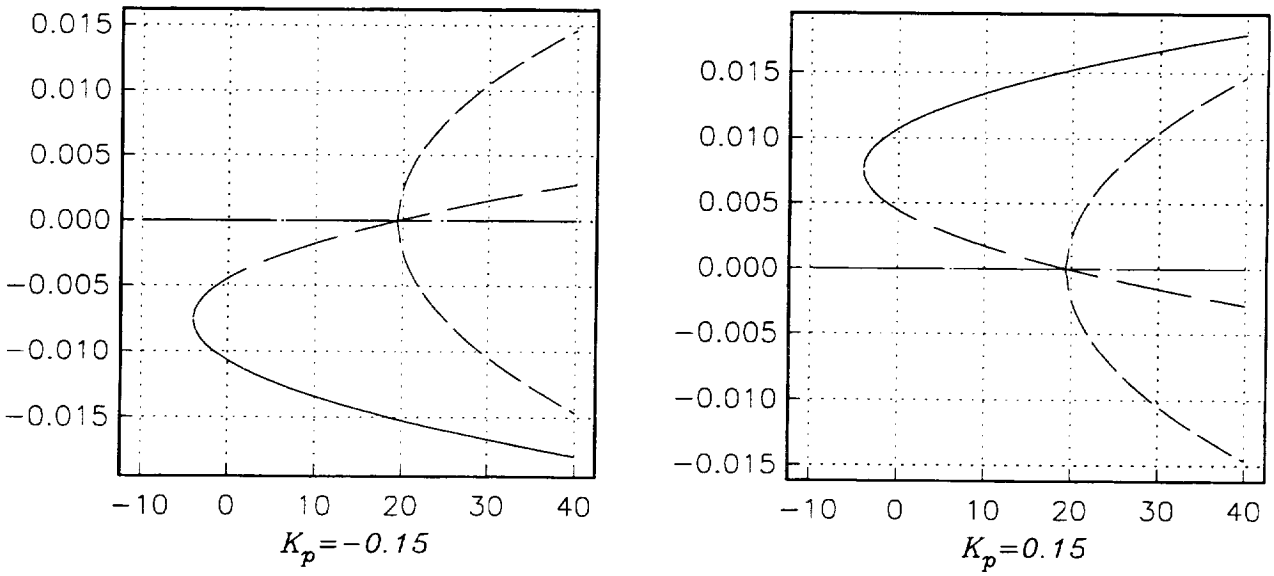

Figure 3: Z_0 vs ϵ for $K_p = \pm 0.15$, K_n=0.0

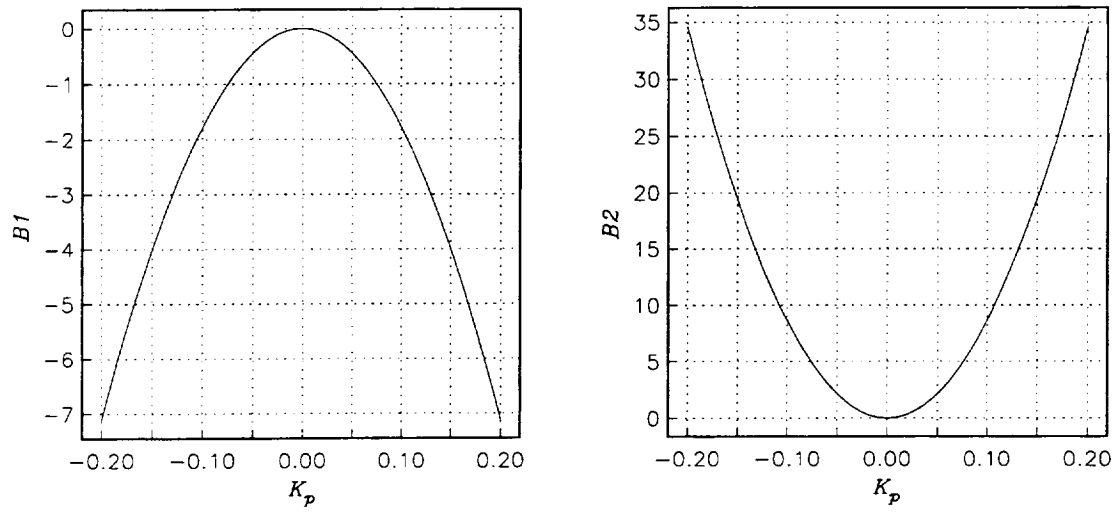

Figure 4: Variation of $B1$ and $B2$ with K_p, K_n=0.0

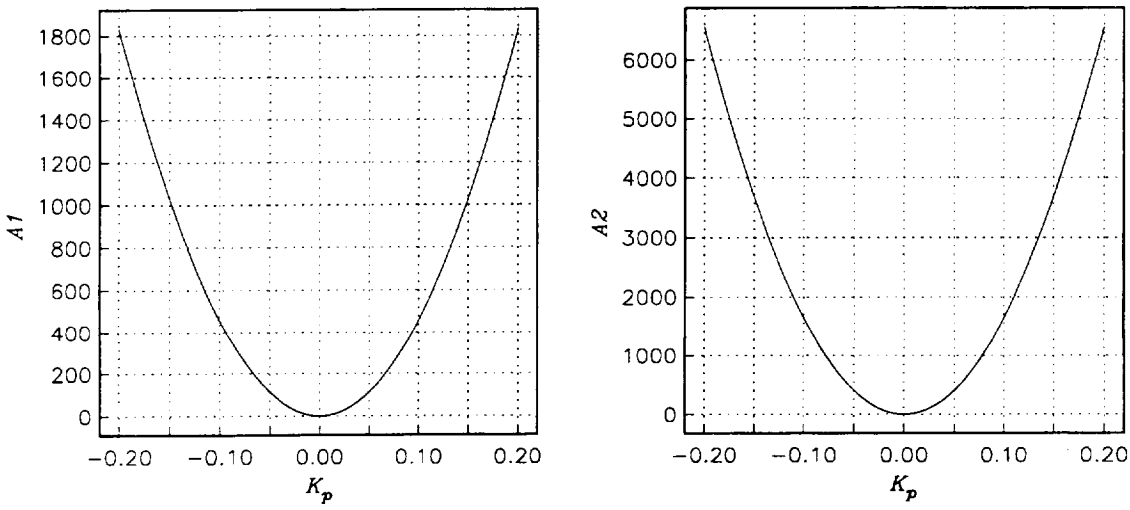

Figure 5: Variation of $A1$ and $A2$ with K_p, K_n=0.0

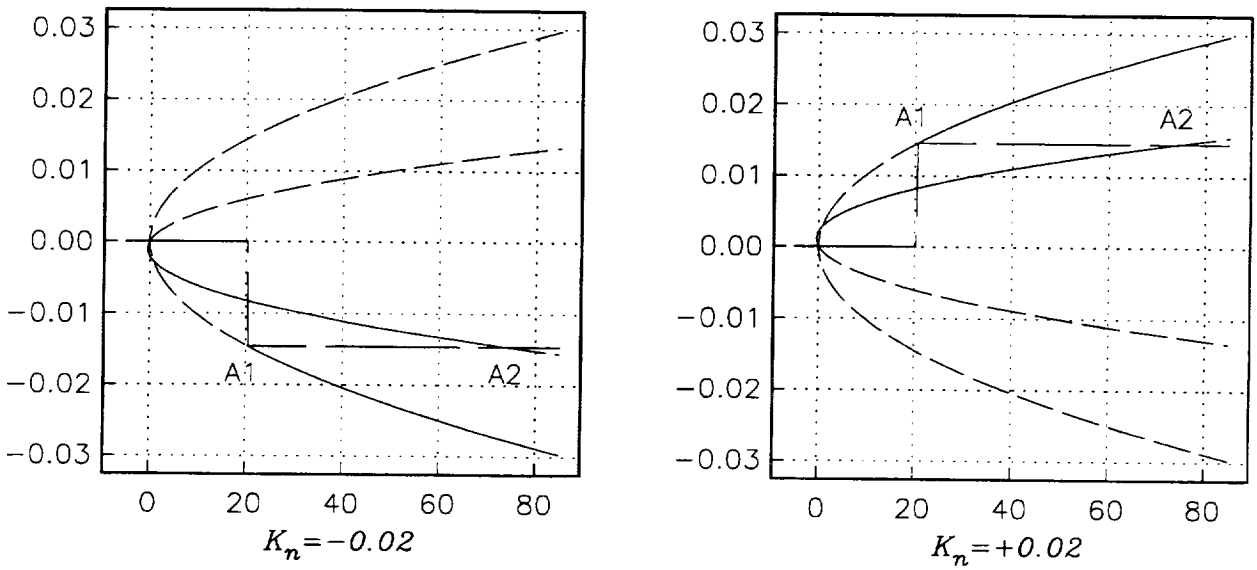

Figure 6: Z_0 vs ϵ for $K_n = \pm 0.02$, K_p=0.0

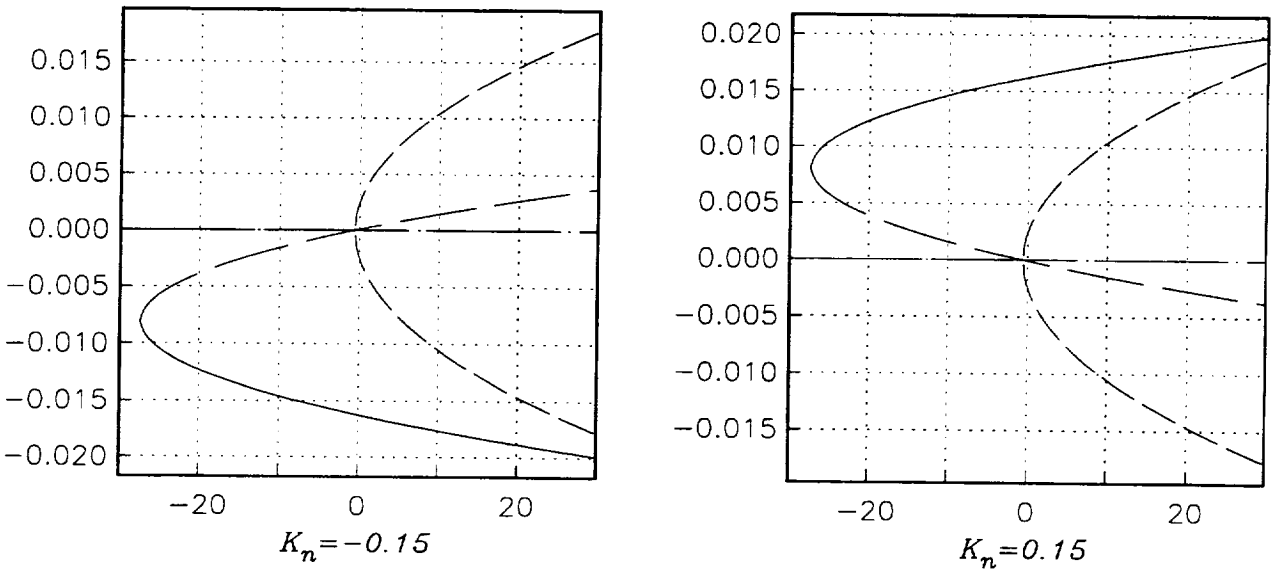

Figure 7: Z_0 vs ϵ for $K_n = \pm 0.15$, K_p=0.0

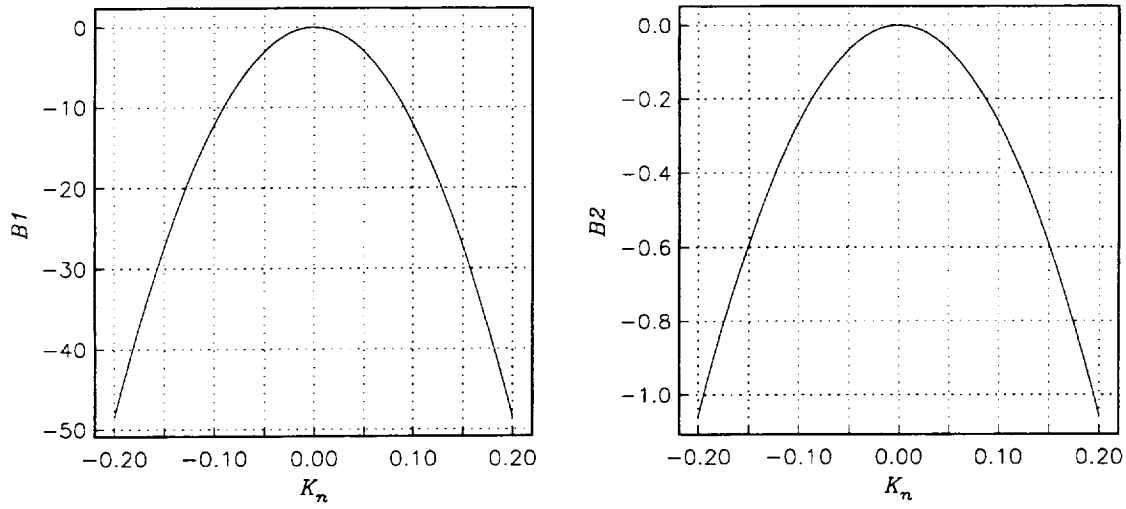

Figure 8: Variation of $B1$ and $B2$ with K_n, K_p=0.0

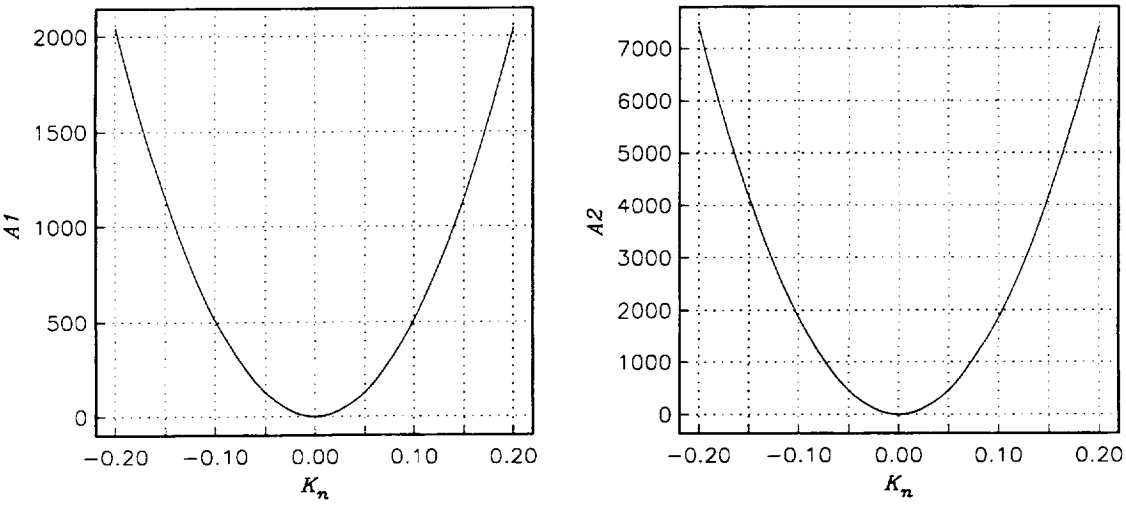

Figure 9: Variation of $A1$ and $A2$ with K_n, K_p=0.0

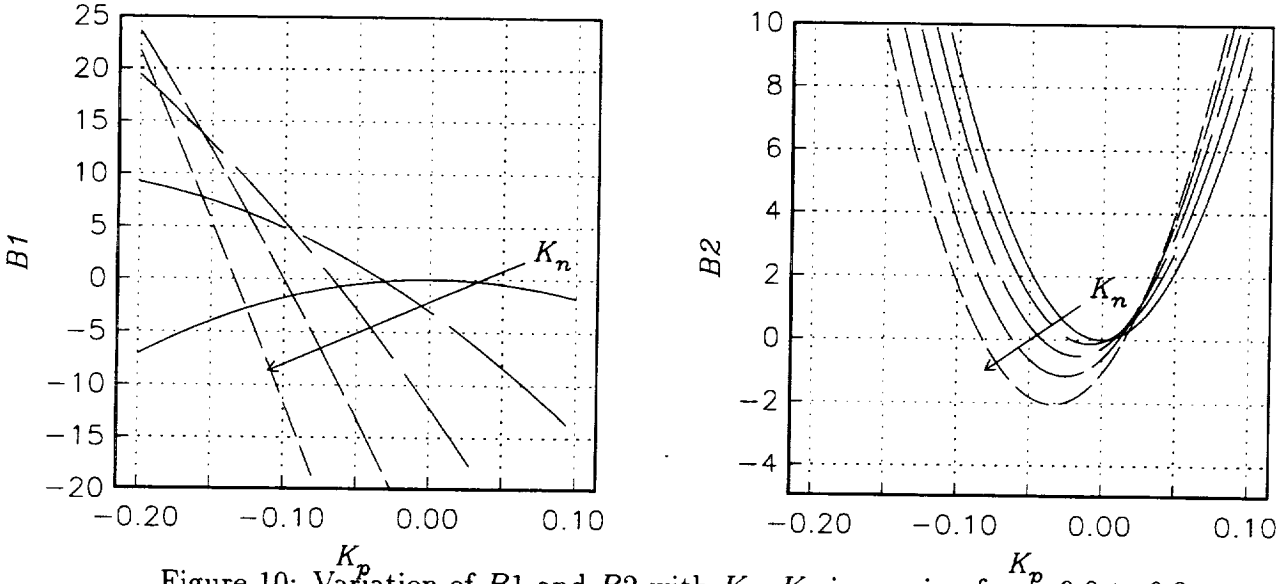

Figure 10: Variation of $B1$ and $B2$ with K_p, K_n increasing fro m 0.0 to 0.2

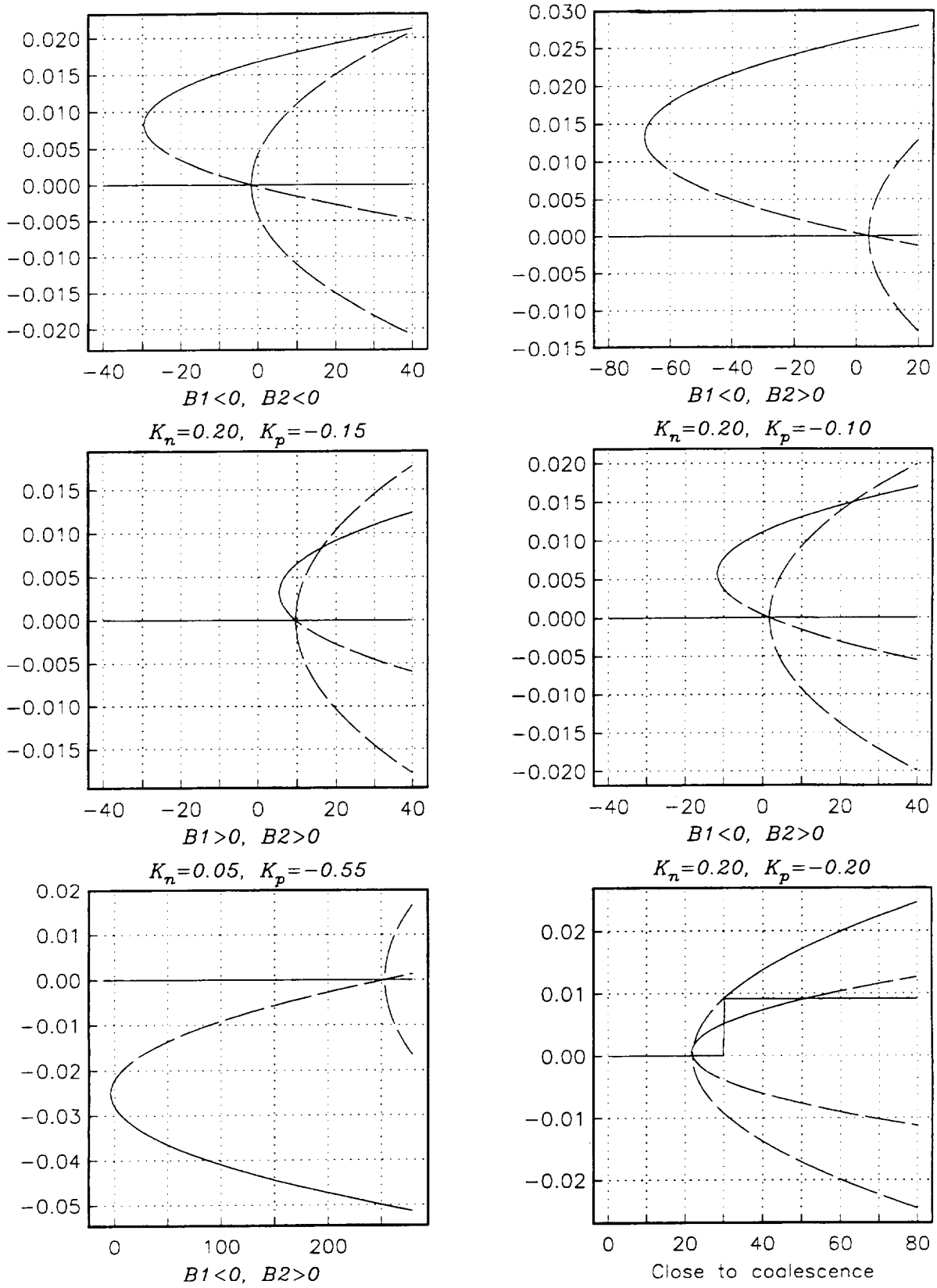

Figure 11: Bifurcation diagrams for a range of K_n and K_p

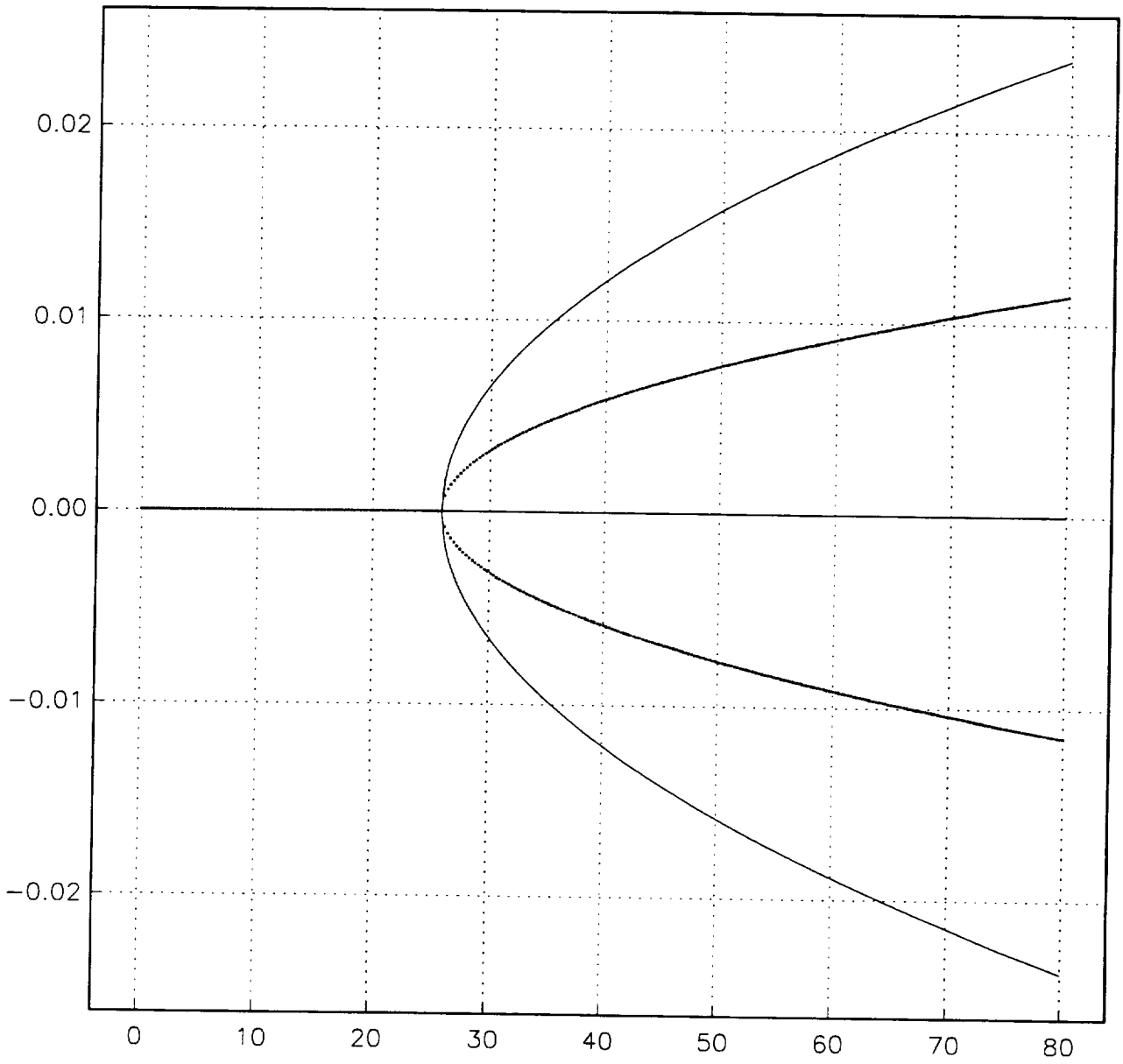

Figure 12: Equilibrium forms for z_0 for a given $K_n = 0.2$ and K_p as given by (2.8a-e)

REPORT DOCUMENTATION PAGE

Form Approved
OMB No. 0704-0188

1. AGENCY USE ONLY *(Leave blank)*	2. REPORT DATE	3. REPORT TYPE AND DATES COVERED
	February 1996	Contractor Report

4. TITLE AND SUBTITLE
ON THE EFFECT OF FEEDBACK CONTROL ON BÉNARD CONVECTION IN A BOUSSINESQ FLUID

5. FUNDING NUMBERS
C NAS1-19480
WU 505-90-52-01

6. AUTHOR(S)
Trudi A. Shortis
Philip Hall

7. PERFORMING ORGANIZATION NAME(S) AND ADDRESS(ES)
Institute for Computer Applications in Science and Engineering
Mail Stop 132C, NASA Langley Research Center
Hampton, VA 23681-0001

8. PERFORMING ORGANIZATION REPORT NUMBER
ICASE Report No. 96-9

9. SPONSORING/MONITORING AGENCY NAME(S) AND ADDRESS(ES)
National Aeronautics and Space Administration
Langley Research Center
Hampton, VA 23681-0001

10. SPONSORING/MONITORING AGENCY REPORT NUMBER
NASA CR-198280
ICASE Report No. 96-9

11. SUPPLEMENTARY NOTES
Langley Technical Monitor: Dennis M. Bushnell
Final Report
Submitted to Phil. Trans. Roy. Soc.

12a. DISTRIBUTION/AVAILABILITY STATEMENT
Unclassified–Unlimited

Subject Category 34

12b. DISTRIBUTION CODE

13. ABSTRACT *(Maximum 200 words)*
The effect of nonlinear feedback control strategies on the platform of convection in a Boussinesq fluid heated from below is investigated. In the absence of the control, given that non-Boussinesq effects may be neglected, it is well known that convection begins in the form of a supercritical bifurcation to rolls. Non-Boussinesq behaviour destroys the symmetry of the basic state, and through a subcritical bifurcation leads to the formation of hexagonal cells. Here we discuss the influence of regulation of the lower surface temperature by means of a control mechanism, made up of a combination of a proportional linear and nonlinear controller, on the stability of the hexagonal cell pattern.

14. SUBJECT TERMS
Feedback Control; Bénard Convection

15. NUMBER OF PAGES
26

16. PRICE CODE
A03

17. SECURITY CLASSIFICATION OF REPORT	18. SECURITY CLASSIFICATION OF THIS PAGE	19. SECURITY CLASSIFICATION OF ABSTRACT	20. LIMITATION OF ABSTRACT
Unclassified	Unclassified		

NSN 7540-01-280-5500

Standard Form 298(Rev. 2-89)
Prescribed by ANSI Std. Z39-18
298-102